A versatile metasurface for meta-nanoprinting and bifocal metalens

Qiangbo Zhang[a], Chang Wang[a], Yan Sun[a], Xinyu Liu[a], Zeqing Yu[a], Fei Wu[b], and Zhenrong Zheng*[a]

[a]College of Optical Science and Engineering, Zhejiang University, Hangzhou 310027, China

[b]Beijing LLVision Technology Co., Ltd., Beijing 100000, China

*Corresponding author: zzr@zju.edu.cn

ABSTRACT

As novel planar structures, the metasurfaces exhibit the unprecedented capability to manipulate the amplitude, phase, and polarization of electromagnetic waves. Therefore, metasurface is designed to apply to metalens, holography, nanoprinting display, encryption, and so on. It is very interesting and meaningful work to integrate bifocal metalens and nanoprinting images into a single metasurface. A method is proposed to combine propagation phase and geometric phase, as well as Malus's law to realize the function of the bifocal metalens and clear nanoprinting display in the near field which can be observed at a certain polarization. This original design expands the functional integration of metasurface and improves applications in image displays, optical storage, augmented reality, virtual reality, and many other related fields.

Keywords: geometric phase, propagation phase, Malus's law, meta-nanoprinting, bifocal metalens

1. INTRODUCTION

Metasurfaces, ultrathin nanostructures composed of plasmonic or dielectric nanoantennas, have aroused the enormous attention owing to their unprecedented capability to manipulate the amplitude, phase, and polarization of electromagnetic waves[1]. The excellent capability of metasurfaces offer lots of applications, such as metalens, hologram, nanoprinting display, encryption, and so on. Recently, the versatile metasurfaces becomes a hot spot due to the unparalleled design freedoms of meta-atoms[2-6]. Li et al. have implemented three-channel metasurfaces for simultaneous meta-holography and meta-nanoprinting[2]. Zhao et al. have realized two pairs of complementary meta-nanoprinting and meta-holography[5]. The versatile metasurfaces to decouple for near- and far-field have been proposed which possess two functions of meta-nanoprinting and metalens[6].

In this paper, we propose a versatile metasurfaces which have functions of meta-nanoprinting and bifocal metalens designed by using geometric phase, propagation phase and Malus's law[2]. Using polarization-dependent geometric phase and Marius formula, a continuous grayscale image can be obtained in the near field of the metasurface. Then use the polarization-independent propagation phase to compensate the geometric phase to obtain two focal points of different lengths in the far field. The above metasurface functions are achieved by different incident polarizations and optical setups as decoding keys. When the polarizer and analyzer are respectively in front of and behind the designed metasurface with suitable polarization angle, a continuous grayscale image will appear in the near field. The designed metasurface will respectively focus incident beams into different focal spots when left circular polarization (LCP) and right circular polarization (RCP) incident.

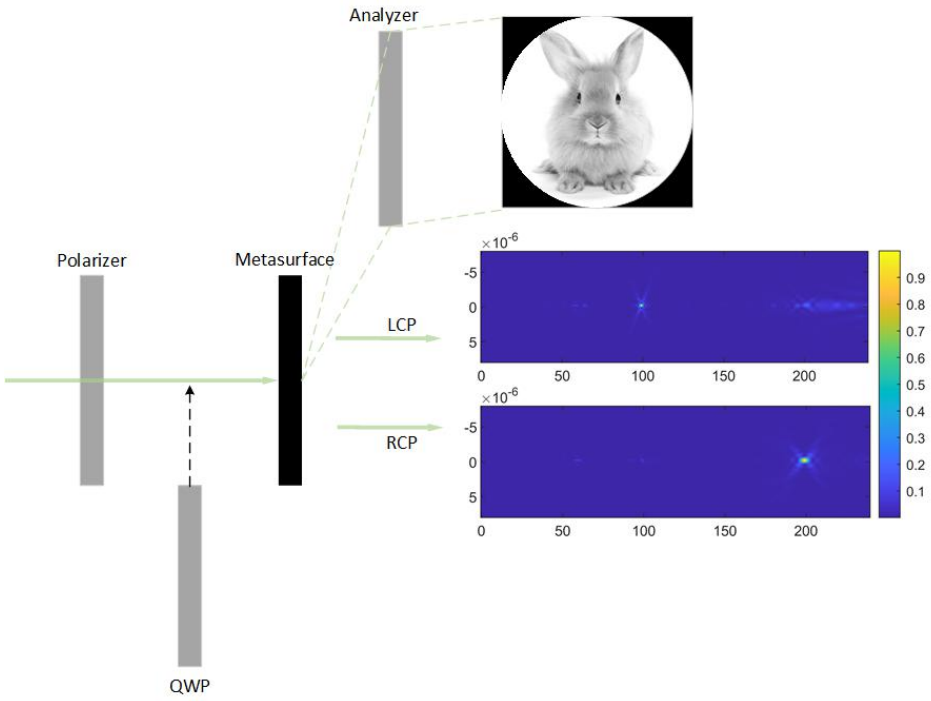

Figure 1. Schematic of the designed three-channel multifunctional metasurface

2. THEORETICAL ANALYSES

2.1 Meta-nanoprinting

As shown in **Figure 1**, our designed metasurface has three-channel for different incident polarizations and optical setups as decoding keys. For the continuous grayscale image, it is implemented by geometric phase and Malus's law. the Jones matrix of the meta-atom can be expressed as

$$J(\alpha)=R(-\alpha)\begin{bmatrix} t_u & 0 \\ 0 & t_v \end{bmatrix}R(\alpha)=\begin{bmatrix} t_u\cos^2\alpha+t_v\sin^2\alpha & (t_u-t_v)\sin\alpha\cos\alpha \\ (t_u-t_v)\sin\alpha\cos\alpha & t_u\sin^2\alpha+t_v\cos^2\alpha \end{bmatrix}, \tag{1}$$

where $R(\alpha)$ is the rotation matrix, t_u and t_v is respectively x- and y-polarization phase shifts of the meta-atom. When the unit light beam with the polarization angle θ_1 is incident on the nanorod, and the analyzer with the polarization angle θ_2 is placed behind the metasurface, the output light beam can be expressed as

$$\begin{bmatrix} E_{xout} \\ E_{yout} \end{bmatrix}=\begin{bmatrix} \cos^2\theta_2 & \sin\theta_2\cos\theta_2 \\ \sin\theta_2\cos\theta_2 & \sin^2\theta_2 \end{bmatrix}J(\alpha)\begin{bmatrix} \cos\theta_1 \\ \sin\theta_1 \end{bmatrix}. \tag{2}$$

Thus, the intensity of the emitted light can be described as

$$I=\left|\left[\frac{t_u-t_v}{2}\cos(2\alpha-\theta_2-\theta_1)+\frac{t_u+t_v}{2}\cos(\theta_2-\theta_1)\right]\right|^2, \tag{3}$$

if θ_2 - $\theta_1=\pi/2$, the second term of the above formula can be eliminated. Then the intensity has a maximum when the meta-atom is selected as perfect half-wave plates (HWP). At this moment, the intensity can be expressed as

$$I=\left|\cos\left(2\alpha-\theta_2-\theta_1\right)\right|^2, \tag{4}$$

set $\theta_1=\pi/4$, $\theta_2=3\pi/4$, then

$$I=\left|\cos\left(2\alpha\right)\right|^2. \tag{5}$$

Therefore, set the polarizer and the analyzer to the corresponding angle, and rotate the nanorod regarded as the half-wave plate according to the above formula, a continuous gray-scale image can be obtained in the near field of metasurface.

2.2 Bifocal Metalens

The phase profile of the bifocal metalens illuminated by an incident plane wave is in the form of[7]

$$\varphi_{(1,2)}(x,y)=-\frac{2\pi}{\lambda}(\sqrt{(x^2+y^2+f_{(1,2)}{}^2}-f_{(1,2)}), \tag{6}$$

where φ_1 and φ_2 are respectively the phase profile of LCP and RCP incident, (x, y) is the location of one arbitrary point on the surface of the bifocal metalens, λ is the working wavelength, f_1 and f_2 are respectively the two focal lengths of the bifocal metalens.

We utilize geometric phase χ and propagation phase ψ to achieve the bifocal metalens. Since the propagation phase ψ is polarization-independent, it can be used as a reference quantity for the phase. The geometric phase χ is polarization-dependent, so when polarized light of different helicity incidents the metasurface, the opposite phase can be generated, which is described as the phase shift. Our bifocal metalens is designed bifocal lens based on the above principles, thus geometric phase χ and propagation phase ψ can be expressed as[2]

$$\chi=\left(\varphi_2-\varphi_1\right)/2, \tag{7}$$

and

$$\psi=\left(\varphi_1+\varphi_2\right)/2. \tag{8}$$

Therefore, $\varphi_1=\psi-\chi$ for the LCP incident, while $\varphi_2=\psi+\chi$ for the RCP incident.

Since the geometric phase is related to the rotation angle of the nanorods, which has been determined by the previous continuous grayscale image in the near field. Therefore, the geometric phase required by the bifocal metalens needs to be approximated, which is specially determined by the four-step geometric phase. The reason for the four-step geometric phase is that the same light intensity corresponds to four rotation angles in the range of 2π according to Eq. Therefore, the rotation angle required for each meta-atom of the bifocal lens selects the closest rotation angle among the four-step geometric phase to achieve the smallest error.

For the propagation phase, we adopt the eight-step propagation phase method. Eight half-wave plate nanorods with different transmission phases interpolated into 0 to 2π uniformly are selected. According to Eq, Eq, the four-step geometric phase and the eight-step propagation phase, the polarization-dependent bifocal metalens can be designed. In theory, the grayscale image in the near field is ideal, while the two focal points in the far field are not ideal due to approximation processing.

3. RESULTS AND DISCUSSIONS

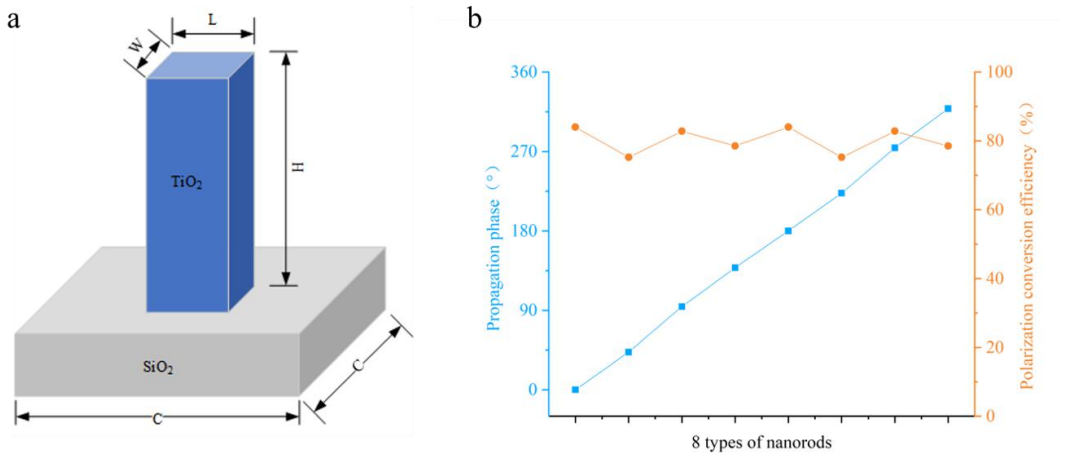

Figure 2. The design and selection of meta-atoms. a) Schematic of the meta-atom. b) The propagation phase and polarization conversion efficiency of the selected eight nanorods.

As shown in **Figure 2a**, the designed meta-atom is composed of a titanium dioxide (TiO_2) nanorod siting on a transparent planar substrate (SiO_2). Simulations using a commercial finite difference time domain (FDTD) solver. The working wavelength is 532 nm. The designed nanorods have a same height (H) of 600 nm, and cell size (C) of 400 nm. The length and width of the nanorod both vary from 50 nm to 300 nm. Then we select the eight nanorods working as HWP. As shown in **Figure 2b** and **Table 1**, the propagation phase of eight nanorods are uniformly distributed between 0 and 2π, and their transmittance exceeds 75%. In addition, the polarization conversion efficiency of eight nanorods are all greater than 99%. Therefore, the selected eight nanorods can be considered ideal HWP.

Table 1. Dimensions of the selected 8 nanorods and their corresponding propagation phases, transmittances and polarization conversion efficiency

nanorods	1	2	3	4	5	6	7	8
Length [nm]	240	290	70	100	110	115	250	215
Width [nm]	110	115	250	215	240	290	70	100
X-Y phase [rad]	3.13	3.04	3.11	3.12	3.15	3.25	3.17	3.16
Propagation phase [rad]	0.00	0.74	1.65	2.42	3.14	3.89	4.79	5.56
Transmittance [%]	84.00	75.22	82.81	78.53	84.01	75.24	82.81	78.52
polarization conversion efficiency [%]	99.82	99.34	99.18	99.03	99.82	99.34	99.18	99.03

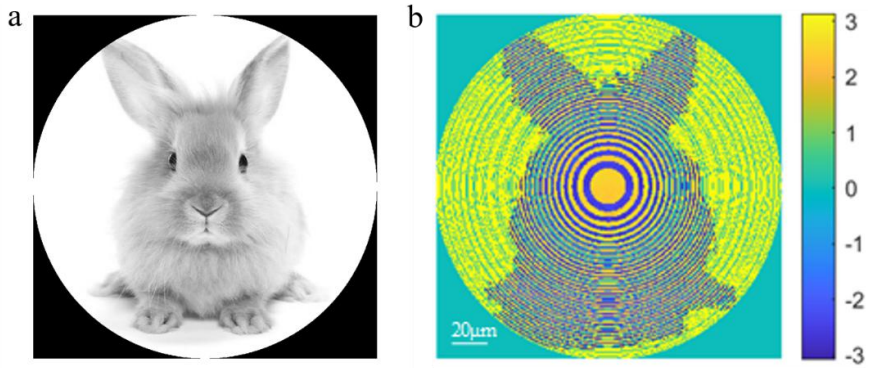

Figure 3. The image of near field and the phase profile of the designed metasurface. a) The simulation result of near-field grayscale image. b) Phase profile on metasurface.

We designed a metasurface of 500 × 500 units, and choose an image of rabbit as the meta-nanoprinting, The four rotation angles of the unit nanorod are initially determine according to the Eq. Then the optimal rotation angle of the

nanorod is determined to meet the minimum error of geometric phase χ according to the Eq. At last, the size of each nanorod is selected from eight selected nanorods which are regarded as half-wave plates. In the eight-step propagation phase, the phase among nanorods closest to the required propagation phase at the corresponding position determines the geometric size of the nanorod at that location. So far, the geometric size and rotation angle of each unit nanorod have been determined. We have obtained an image of a rabbit in the near field of metasurface and achieved the polarization-dependent bifocal metalens through simulation as shown in **Figures 3-4**. Here, we assume that the various unit structures of the metasurface do not affect each other. Each pixel of the final near-field image is an independent result produced by the incident light once passing through the polarizer, metasurface, and analyzer.

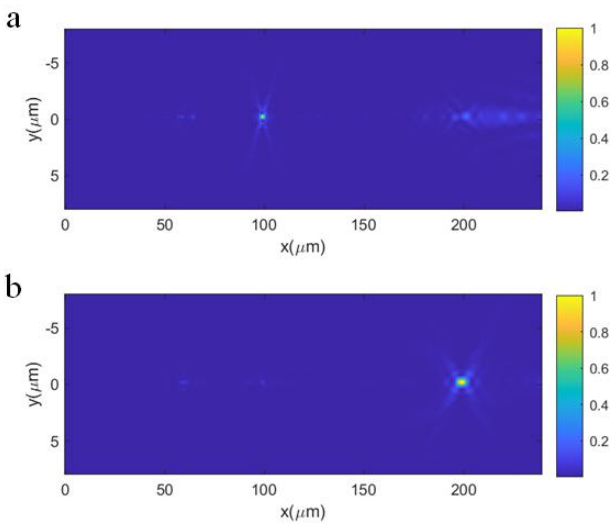

Figure 4. The simulated electric field ($|E|^2$) distributions in the x-z plane of the polarization-dependent bifocal metalens. a-b) The simulated electric field ($|E|^2$) distributions with LCP incident(a) and RCP incident(b).

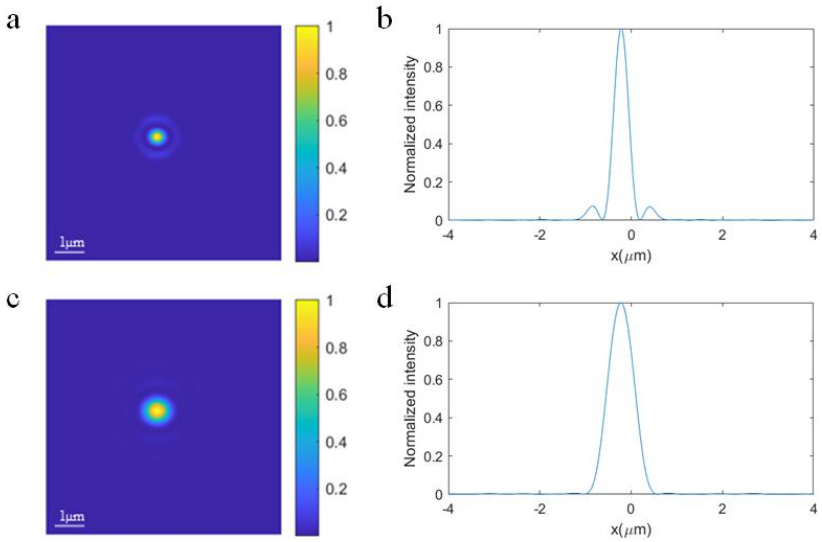

Figure 5. The simulated focal spots of designed bifocal metalens. a) The simulated electric field ($|E|^2$) distributions of focal spot in the x-y plane with LCP incident. b) The normalized energy along the x axis at the focal spot with LCP incident. c) The simulated electric field ($|E|^2$) distributions of focal spot in the x-y plane with RCP incident. d) The normalized energy along the x axis at the focal spot with RCP incident.

We design the polarization-dependent bifocal metalens with 100 μm of LCP incident and 200 μm of RCP incident, and their corresponding numerical aperture (NA) are respectively 0.71 and 0.45. The simulated electric field (|E|2) distributions in the x-y and in the x-z plane are respectively shown in Figures 4-5. The full width at half maximum

(FWHM) of the two focal points obtained by simulation are respectively 360 nm and 600 nm for LCP and RCP incident. However, the focusing efficiencies of the bifocal metalens are very low, only 3.7% and 6.3% for LCP and RCP incident. The main reason for the low focusing efficiency is that the multi-functional metasurface we designed is in principle to meet the ideal near-field image, and for this reason, the far-field bifocal effect has been greatly sacrificed. This results in that the phase profile on the metasurface is not an ideal lens phase profile, so this leads to a very low convergence efficiency of the final bifocal metalens.

According to the simulation results, the designed metasurface has a very ideal near field and an imperfect double focus spots, which is consistent with the principle analysis.

4. CONCLUSIONS

In summary, an approach to design a versatile metasurface for meta-nanoprinting and bifocal metalens is proposed and numerically demonstrated. Finally, through our design, we simulated an ideal near-field continuous grayscale image and a sacrificed polarization-dependent bifocal metalens. How to improve the focusing efficiency of the bifocal metalens to achieve a more ideal multifunctional metasurface will become the goal of our next work. This original design expands the functional integration of metasurface and improves applications in image displays, optical storage, augmented reality, virtual reality, and many other related fields.

REFERENCES

[1] Yu, N., and Capasso, F., "Flat optics with designer metasurfaces," Nature Materials. 13(2), 139-150 (2014).

[2] Li, Z. L., Chen, C., Guan, Z. Q., Tao, J., Chang, S., Dai, Q., Xiao, Y., Cui, Y., Wang, Y. Q., Yu, S. H., Zheng, G. X. and Zhang, S., "Three-Channel Metasurfaces for Simultaneous Meta-Holography and Meta-Nanoprinting: A Single-Cell Design Approach," Laser & Photonics Reviews. 14(6), 2000032 (2020).

[3] Dai, Q., Guan, Z., Chang, S., Deng, L., Tao, J., Li, Z., Li, Z., Yu, S., Zheng, G. and Zhang, S., "A Single‐Celled Tri‐Functional Metasurface Enabled with Triple Manipulations of Light," Advanced Functional Materials. 30(50), 2003990 (2020).

[4] Juan, D., Deng, L., Guan, Z., Tao, J., Li, G., Li, Z., Li, Z., Yu, S. and Zheng, G., "Multiplexed Anticounterfeiting Meta-image Displays with Single-Sized Nanostructures," Nano Letters. 20(3), 1830-1838 (2020).

[5] Zhao, R., Xiao, X., Geng, G., Li, X., Li, J., Li, X., Wang, Y. and Huang, L., "Polarization and Holography Recording in Real- and k-Space Based on Dielectric Metasurface," Advanced Functional Materials. 31(27), 2100406 (2021).

[6] Li, J., Wang, Y., Chen, C., Fu, R., Zhou, Z., Li, Z., Zheng, G., Yu, S., Qiu, C.-W. and Zhang, S., "From Lingering to Rift: Metasurface Decoupling for Near- and Far-Field Functionalization," Advanced Materials. 33(16), 2007507 (2021).

[7] Khorasaninejad, M., Chen, W.T., Devlin, R.C., Oh, J., Zhu, A.Y. and Capasso, F., "Metalenses at visible wavelengths: Diffraction-limited focusing and subwavelength resolution imaging," Science. 352(6290), 1190-1194 (2016).